

# A Direct Method for the Evaluation of Lower and Upper Bound Ratchet Limits

J. Ure<sup>a</sup>, H. Chen<sup>a</sup>, T. Li<sup>a</sup>, W. Chen<sup>a</sup>, D. Tipping<sup>b</sup>, D. Mackenzie<sup>a</sup>

<sup>a</sup>*Dept of Mechanical Engineering, University of Strathclyde, Glasgow, Scotland, G1 1XJ*

<sup>b</sup>*Central Engineering Support, Existing Nuclear, EDF Energy, Barnwood, Gloucester, GL4 3RS*

---

## Abstract

The calculation of the ratchet limit is often vital for the assessment of the design and integrity of components which are subject to cyclic loading. This work describes the addition of a lower bound calculation to the existing Linear Matching Method upper bound ratchet analysis method. This lower bound calculation is based on Melan's theorem, and makes use of the residual and elastic stress fields calculated by the upper bound technique to calculate the lower bound ratchet limit multiplier. By doing this, the method combines the stable convergence of the upper bound method but retains the conservatism offered by the lower bound. These advantages are also complemented by the ability of the Linear Matching Method to consider real 3D geometries subject to complex load histories including the effect of temperature dependent yield stress.

The convergence properties of this lower bound ratchet limit are investigated through a benchmark problem of a plate with a central hole subject to cyclic thermal and mechanical loads. To demonstrate the effectiveness of the method, the ratchet limit of a thick walled pipe-pipe intersection, also subject cyclic thermal and mechanical loads, is considered. Validation of these results is provided by full elastic-plastic FEA in ABAQUS.

*Keywords:* Ratchet limit, shakedown limit, lower and upper bound, cyclic loading

---

## 1. Introduction

During operation under cyclic loading conditions, a structure will show one of three behaviours: shakedown, reversed plasticity (or plastic shakedown) and ratcheting. Ratcheting, the accumulation of strain with each load cycle, is banned by all pressure vessel design codes and therefore must be designed against [1]. Knowledge of the ratchet boundary is also desirable where the structure includes acute stress raisers, such as cracks, which violate the shakedown condition. With these factors in mind, it is highly desirable to be able to calculate the ratchet limit of a structure.

The calculation of the ratchet limit has been studied by many researchers. The complex nature of the ratcheting mechanism means that closed form analytical solutions are restricted to the simplest situations.

Incremental Finite Element Analysis (FEA) can only predict if shakedown, reversed plasticity or ratcheting occur, and so a trial and error process is required to determine the shakedown and ratchet boundaries. As a result of this, many direct methods have been developed which can calculate the shakedown limit of a structure [2-5]. The Linear Matching Method (LMM) has been extended beyond most other direct methods to include calculation of the ratchet limit [6,7]. The current method has been implemented successfully in ABAQUS through user subroutines, and is capable of calculating the shakedown and ratchet limits of structures with complex load histories and temperature dependent yield stress.

However, the existing ratchet analysis method only provides upper bound limits. This work describes the addition of a lower bound analysis which is based on the stress solutions generated by the upper bound calculation. Implementing the lower bound in this way means that the stable convergence offered by the upper bound is retained, but is still complemented by the conservatism of a lower bound solution.

## 2. The Linear Matching Method

Consider a body of volume  $V$  and surface area  $S$ . A cyclic temperature history  $\theta(x_i, t)$  acts within the volume and varying mechanical loads  $P(x_i, t)$  act on part of the surface  $S_T$ . The remainder of the surface is constrained to have zero displacement rate. These loads act over a time cycle of  $0 \leq t \leq \Delta t$ , and can be decomposed into their constant and cyclic components:

$$F(x_i, t) = \lambda \bar{F}(x_i) + \theta(x_i, t) + P(x_i, t) \quad (1)$$

Where  $\lambda$  is a load parameter,  $\bar{F}(x_i)$  is a constant load distribution and  $\theta(x_i, t)$  and  $P(x_i, t)$  are the cyclic history of thermal and mechanical over time  $\Delta t$ . The linear elastic stress history associated with these loads is:

$$\hat{\sigma}_{ij}(x_k, t) = \lambda \hat{\sigma}_{ij}^{\bar{F}} + \hat{\sigma}_{ij}^{\Delta}(x_k, t) \quad \text{where} \quad \hat{\sigma}_{ij}^{\Delta} = \hat{\sigma}_{ij}^P + \hat{\sigma}_{ij}^{\theta} \quad (2)$$

Where  $\hat{\sigma}_{ij}^{\Delta}$  represents the varying stresses due to  $P(x_i, t)$  and  $\theta(x_i, t)$ . The load parameter  $\lambda$  allows a range of loading histories to be considered. For this cyclic problem definition, the stresses and strain rates will asymptote to a steady cyclic state where

$$\sigma_{ij}(t) = \sigma_{ij}(t + \Delta t), \quad \dot{\epsilon}_{ij}(t) = \dot{\epsilon}_{ij}(t + \Delta t) \quad (3)$$

This stress state can be decomposed into three components as shown below in equation 4: the elastic solution  $\hat{\sigma}_{ij}$ , the transient solution accumulated up to the beginning of the cycle,  $\bar{\rho}_{ij}$ , and a residual solution which represents the changes during the cycle  $\rho_{ij}^r$ .

$$\sigma_{ij}(x_k, t) = \hat{\sigma}_{ij}(x_k, t) + \bar{\rho}_{ij}(x_k) + \rho_{ij}^r(x_k, t) \quad (4)$$

For a stable cyclic solution there is no accumulation of stress or strain from one cycle to the next, and therefore:

$$\rho_{ij}^r(x_k, 0) = \rho_{ij}^r(x_k, \Delta t) = 0 \quad (5)$$

Based on this stable cyclic formulation, the evaluation of the ratchet limit becomes possible if the applied loading can be decomposed into constant and varying components. Because the structure is subjected to stable cyclic load conditions, the changing residual stress  $\rho_{ij}^r$  is caused directly by this cyclic load. The constant residual stress field  $\bar{\rho}_{ij}$  caused by the constant loading can then be evaluated after the changing residual stress field has been computed.

The calculation of the ratchet limit consists of two minimization processes. The first is an incremental minimization for the evaluation of the cyclic history of residual stress and plastic strain range. The second is a global minimization for the ratchet limit due to an extra constant load. In essence, once the stable

response of the structure to the cyclic loading is determined, the LMM calculates the maximum additional constant loading which will not cause the component to ratchet.

### 2.1. Upper Bound Formulation

The upper bound formulation of the LMM has been described in detail in other works [6,7]. A brief outline is given here as an introduction to the lower bound calculation.

Once the residual stress history associated with the cyclic component of the applied loading has been determined, the problem reduces to a traditional shakedown analysis where the linear elastic solution is augmented by this varying residual stress field. This shakedown analysis is based on Koiter's upper bound theorem [8]. This theorem states that if 1) any kinematically admissible strain rate can be found such that the strain field is compatible with the applied displacements and 2) that the plastic dissipation within the body is less than or equal to the applied work, then shakedown does not occur.

The upper bound procedure of the LMM uses linear elastic solutions for the applied loads, the load history being constructed within the user subroutine. Using superposition, the total linear elastic stress at each load instance in the cycle is calculated. At the points where this stress is greater than the yield stress, the young's modulus is reduced. Subsequent iterations then use the modified shear modulus from the previous iteration, which allows the stresses to redistribute in the structure. In parallel with the reducing shear modulus, the applied constant load is also scaled using the multiplier,  $\lambda^{UB}$ , which gives the stress field of equation 6. At the end of each iteration, the appropriate energy totals are calculated to determine the upper bound ratchet limit multiplier  $\lambda^{UB}$  which is to be used in the next iteration. The combination of the modified modulus and the load multiplier produces an unambiguous upper bound ratchet limit for the applied loading.

$$\sigma_{ij}(x_k, t) = \lambda^{UB} \hat{\sigma}_{ij}^{\bar{F}} + \hat{\sigma}_{ij}^{\Delta}(x_k, t) + \rho_{ij}(x_k, t) \quad (6)$$

### 2.2. Lower Bound Calculation

Melan's theorem states that for a given load set the structure will exhibit shakedown if a constant residual stress field can be found such that for any combination of cyclic elastic and residual stresses the yield condition is not violated [9]. The evaluation of the ratchet limit described here is essentially a shakedown assessment augmented by the changing residual stress field. This means that Melan's shakedown theorem can be extended to the assessment of the ratchet limit if the stresses used in its calculation include the changing residual stress, where the stress is compared to the temperature dependent yield stress to give the lower bound ratchet multiplier.

In terms of the LMM, the stress solutions calculated in stage 2 of the upper bound method compared with the temperature dependent yield condition:

$$\lambda^{LB} = \frac{\sigma_y(T)}{\lambda^{UB} \hat{\sigma}_{ij}^{\bar{F}} + \hat{\sigma}_{ij}^{\Delta}(x_k, t) + \rho_{ij}(x_k, t)} \quad (7)$$

Numerically, this means that the yield stress of each integration point is divided by the effective stress at that point to obtain the local  $\lambda^{LB}$ . The minimum  $\lambda^{LB}$  calculated from the entire model is used as the lower bound ratchet multiplier. It is worth noting that the yield stress used in this comparison is the local yield stress at that integration point, and therefore temperature dependent yield stress can be used in the calculation. This gives the lower bound stress field:

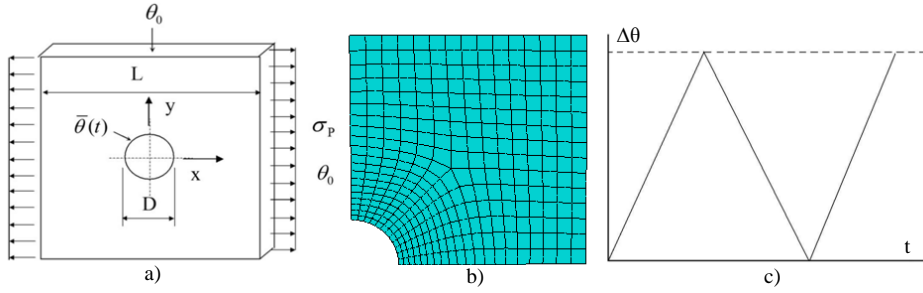


Figure 1 - Holed Plate a) Geometry b) Mesh and c) Cyclic Thermal Load

$$\hat{\sigma}_{ij} = \lambda^{LB} \left( \lambda^{UB} \hat{\sigma}_{ij}^{\bar{F}} + \hat{\sigma}_{ij}^{\Delta}(x_k, t) + \rho_{ij}(x_k, t) \right) \quad (8)$$

### 3. Numerical Examples

#### 3.1. Plate with Central Hole

Figure 1 shows a schematic of the plate geometry and the finite element mesh used. A quarter model is used with appropriate symmetry boundary conditions. The ratio between the diameter of the hole  $D$  and the length of the plate  $L$  is 0.2. The ratio between the thickness  $T$  and the length  $L$  is 0.05. The element type selected for this model was ABAQUS type C3D20R, a 20-node quadratic brick element with reduced integration. The top and right surfaces of the plate are constrained to remain in-plane when displaced. The plate is subject to a constant uniaxial tension,  $\sigma_p$ , along one side of the plate and a cyclic temperature difference between the bore of the hole and the edge of the plate,  $\Delta\theta$ .

The converged upper and lower bound ratchet limits are shown in the interaction diagram in Figure 2a. The thermal stress is normalised against the reference thermal stress at  $\Delta\theta = \Delta\theta_0 = 100^\circ\text{C}$ . For clarity the reverse plasticity limit (also calculated by the LMM) is shown in the figure and thus shows the load domains where the plate will exhibit different cyclic behaviour.

The ratchet limit curve follows the classic bree-like form, and the lower and upper bounds converge very closely. The maximum difference between the lower and upper bound in this example is less than 2%. Figure 2b shows the convergence of the lower and upper bounds at the point A. The upper bound converges quickly to the final solution, owing to the fact that the stress concentration at the hole is

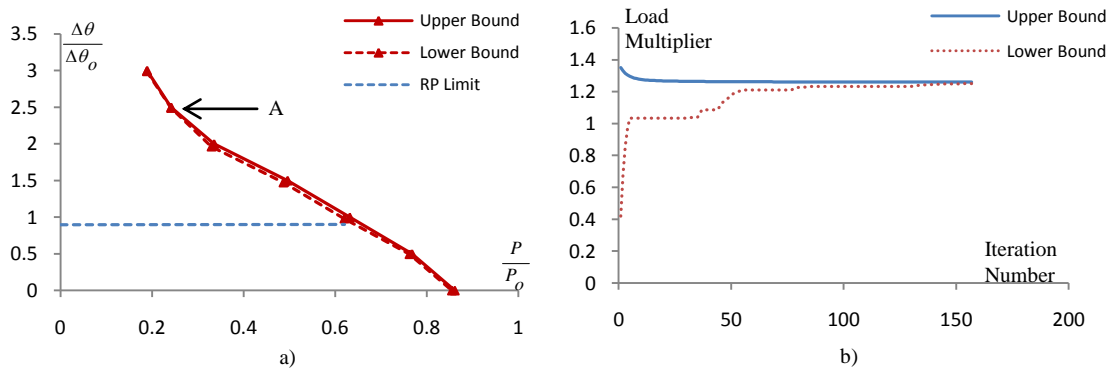


Figure 2 - Results for Holed Plate a) Interaction Diagram and b) Convergence of Point A

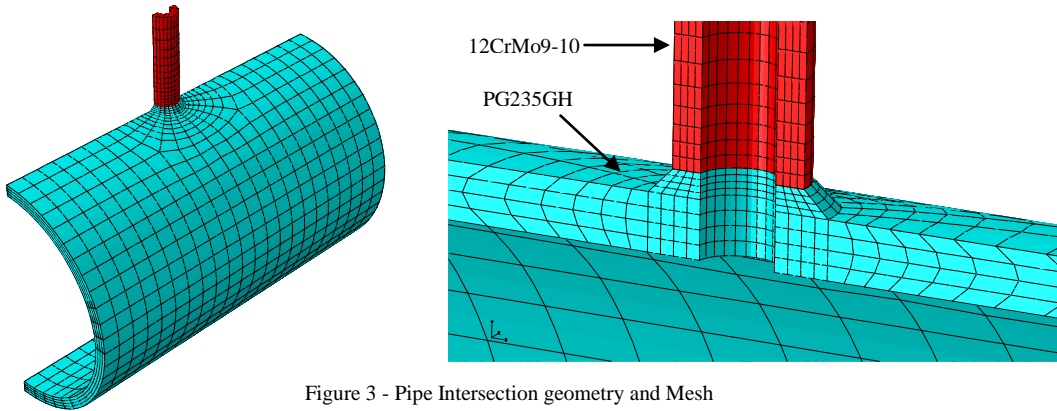


Figure 3 - Pipe Intersection geometry and Mesh

averaged out over the whole volume. The lower bound converges more slowly, because this high stress is the limiting factor of the lower bound calculation.

### 3.2. Pipe Intersection

Figure 3 shows a diagram of the pipe intersection and the FE mesh used. This geometry is taken from the EPERC Design-by-Analysis [10] and, due to symmetric loading, half symmetry is used in the model. ABAQUS element DC3D20 was used for the thermal analysis and ABAQUS element C3D20R was used for the structural analysis.

The pipe intersection is made from two materials. The main pipe is PG235GH and the small pipe is 12CrMo9-10. The small pipe is modelled as being "set-on", and so the weld region has the same material properties as the main pipe. Both temperature dependent and independent analyses are presented with temperature dependent yield stresses being taken from BSEN 10028-2009 [11]. In both cases a temperature independent Young's modulus and thermal expansion coefficient is used.

The pipe intersection is subject to a constant internal pressure,  $P$  (with the closed end condition) and cyclic temperature difference between the inner and outer surfaces,  $\Delta\theta$ . The temperature varies linearly from ambient temperature at the outer surface to  $\Delta\theta$  at the inner surface. This thermal load is cycled in the same way as that of the thermal loading applied to the holed plate. One end of the main pipe is constrained axially and the free ends of both pipes are constrained to expand in-plane, which replicates the expansion of long pipes.

The ratchet interaction diagrams for temperature dependent and independent yield stress are given in

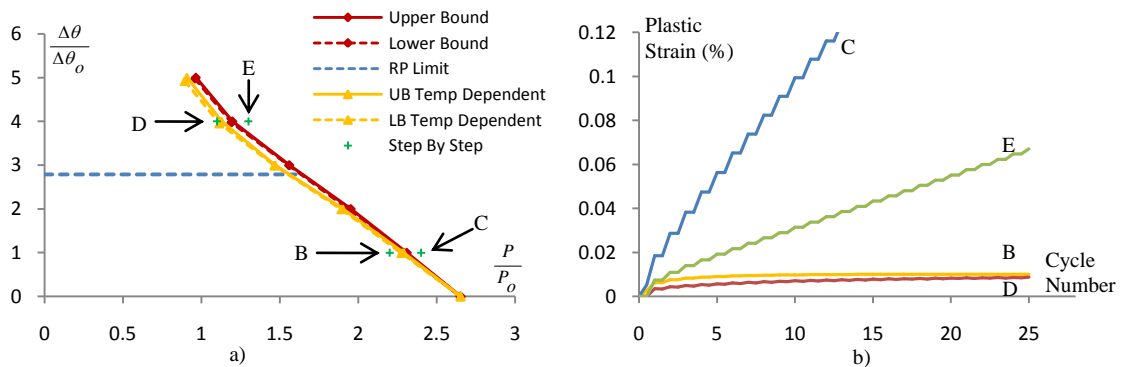


Figure 4 - Pipe Intersection Results a) Interaction Diagram b) Plastic Strain from Full Elastic-Plastic FE at Points B, C, D and E

Figure 4a. The cyclic thermal load is normalised against the initial applied  $\Delta\theta$  of 100°C and the constant internal pressure is normalised against the initial applied pressure of 10MPa. The temperature independent reverse plasticity limit calculated by the LMM shakedown method is included for clarity. Once again the lower and upper bound limits have converged very close to one another.

Figure 4a shows that, with the material properties used, temperature dependency does not have a significant effect on the ratchet interaction diagram. The temperature independent ratchet curve has been validated by four full elastic plastic finite element analyses. The plots of plastic strain (PEMAG) against number of cycles for these points are shown in Figure 4b. Point B, just inside the boundary, shows shakedown behaviour whilst the point C, just outside the boundary, shows clear ratcheting behaviour. A similar situation is observed with points D and E which show reversed plasticity and ratcheting behaviour respectively.

#### 4. Conclusion

The linear Matching Method has been proven to give accurate bounds to shakedown and ratcheting of components subject to cyclic loading. With the addition of the lower bound to the current ratchet analysis method, it is now possible to calculate an accurate yet conservative ratchet bound. This is a powerful tool to engineers involved in the assessment and design of structural components.

#### Acknowledgements

The authors would like to thank the Engineering and Physical Sciences Research Council (EPSRC) of the United Kingdom, EDF Energy and The University of Strathclyde for their support during this work.

#### References

- [1] British Energy Generation Ltd. R5, An Assessment Procedure for the High Temperature Response of Structures, Issue 3, 2003.
- [2] Mackenzie D, Boyle JT, Hamilton R. The elastic compensation method for limit and shakedown analysis: a review. *Journal of Strain Analysis* 2000;**35**(3):171-188
- [3] Seshadri R. Inelastic evaluation of mechanical and structural components using the generalized local stress strain method of analysis. *Nuclear Engineering and Design* 1995;**153**:287-303
- [4] Muscat M, Mackenzie D, Hamilton R. Evaluating shakedown under proportional loading by non-linear static analysis. *Computers and Structures* 2003;**81**:1727-1737
- [5] Chen H. Lower and upper bound shakedown analysis of structures with temperature dependent yield stress. *Journal of Pressure Vessel Technology* 2010;**132**:011202 1-8
- [6] Chen H, Ponter ARS. A direct method on the evaluation of ratchet limit. *Journal of Pressure Vessel Technology* 2010;**132**:041202 1-8
- [7] Chen H, Ponter ARS. A method for the evaluation of a ratchet limit and the amplitude of plastic strain for bodies subjected to cyclic loading. *Eur J Mech A/Solids* 2001;**20**:555-571
- [8] Koiter WT. General theorems for elastic plastic solids. *Progress in solid mechanics*, Sneddon JN and Hill R, eds., North Holland, Amsterdam 1960;**1**:167-221
- [9] Melan E. Theorie statisch unbestimmter systeme aus ideal-plastischem baustoff. *Sitzungsber. d. Akad. d. Wiss.* 1936;Wien **2A**(145):195-218
- [10] European Pressure Equipment Research Council. Design by analysis manual 1999.
- [11] British Standards Institute. BS EN 10028-2:2009, Flat products made of steel for pressure purposes.